Check for updates

Received: 8 October 2022 | Accepted: 3 November 2022

DOI: 10.1002/pamm.202200206

Aspects of accuracy and uniqueness of solutions in data-driven mechanics

Thorsten Bartel[1,*], **Marius Harnisch**[1], **Andreas Menzel**[1,2], and **Ben Schweizer**[3]

[1] Institute of Mechanics, Department of Mechanical Engineering, TU Dortmund, Germany
[2] Division of Solid Mechanics, Department of Construction Sciences, Lund University, Sweden
[3] Department of Mathematics, TU Dortmund, Germany

Data-driven methods provide great potential for future applications in engineering, for example in terms of more efficient simulations. Conventional material models and the associated constitutive equations are substituted by a minimization of a distance between so-called material and mechanical states, which, however, leads to non-unique solutions. The aim of this paper is to analyze the influence of the chosen initial values on the accuracy of the obtained results. Furthermore, Mixed Integer Quadratic Programming (MIQP) is implemented and its applicability to data-driven mechanics is assessed.

© 2023 The Authors. *Proceedings in Applied Mathematics & Mechanics* published by Wiley-VCH GmbH.

1 Introduction

Data-driven mechanics represents a promising evolution step in the modeling and simulation of complex material behavior. It relies on experimental mechanics and conventional material modeling, avoiding the significant drawbacks of the latter. To be more precise, the implementation of conventional constitutive models for complex material behavior (mostly in terms of the Finite Element Method) — even for purely elastic behavior — is often too time-consuming. This becomes particularly apparent when considering the coupling between simulations of complex processes and their direct control, such as in manufacturing processes.

The foundation for data-driven elasticity was built by [1], where compatible displacement fields and divergence-free stress fields are linked to each other by data sets rather than direct functional relations. This concept has been adopted and extended by several scientists: The authors [2] use manifold learning methodologies in order to extract the most relevant information stored in data sets with the aim of reducing their sizes. The authors [3] extend their own method with the capability to use noisy data and [4] introduce a data-driven mechanics formulation for dynamic problems. In [5] the so-called Data-Driven Identification Method is developed, in which data sets are generated based on Digital Image Correlation. How to design appropriate experiments for finding optimal constitutive models by using data-driven algorithms is discussed in [6]. An extension in terms of large deformations is presented in [7] together with the introduction of a Two-Field formulation. A mathematical treatise of the new concept including convergence analysis and notions of relaxation is provided in [8] for linear elasticity and in [9] for nonlinear elasticity. The authors [10] established a different methodology with the aim to enhance accuracy and robustness of the data-driven approach against noise and outliers by using the so-called Reproducing Kernel Particle Method in conjunction with the Stabilized Conforming Nodal Integration scheme. Data-driven multiscale approaches are treated in [11] and [12], which significantly increase the computing efficiency of scale-bridging numerical homogenization methods such as FE^2 formulations according to [13]. Forays into the application of data-driven mechanics to inelastic material behavior have been been achieved by [14] and [15], among others. In this context, [16] present a sophisticated methodology to address the involved challenges by using a neural network to capture the material's history.

The aim of this paper is to quantitatively analyze the influence of chosen initial values in terms of the so-called material states on the accuracy of obtained results. Furthermore, a specific Mixed Integer Quadratic Programming (MIQP) algorithm has been implemented, the results of which serve as reference solution. However, severe drawbacks of this method are figured out as well. Aspects of accuracy and non-uniqueness of solutions that are obviously caused by the staggered scheme have already been pointed out by, e.g., [17]. In [18] the data sets are enhanced with locally linear tangent spaces in an offline step to improve convergence and accuracy. However, a detailed treatise on the impact of the chosen initial values is so far missing in literature.

The structure of the present paper is as follows: Section 2 includes the basics of the original approach and the related algorithm. In section 3, three different case studies are considered. Results obtained by the conventional staggered minimization routine are analyzed in terms of accuracy and also compared to results obtained by MIQP. In section 4, the essential conclusions of the present paper are summarized and an outlook on future objectives is given.

2 Original approach

In this section, the framework of data-driven linear elasticity as introduced in [1] shall be briefly discussed. The essential equations of the original approach are shown and the essential steps of the algorithm are explained.

* Corresponding author: e-mail thorsten.bartel@udo.edu, phone +49-231-755 2668,

This is an open access article under the terms of the Creative Commons Attribution-NonCommercial-NoDerivs License, which permits use and distribution in any medium, provided the original work is properly cited, the use is non-commercial and no modifications or adaptations are made.

2.1 Basic relations

The cornerstone of data-driven mechanics is the data-set

$$\mathcal{D}_{\mathrm{loc}} := \left\{ (\widetilde{\boldsymbol{\varepsilon}}, \widetilde{\boldsymbol{\sigma}})_1, (\widetilde{\boldsymbol{\varepsilon}}, \widetilde{\boldsymbol{\sigma}})_2, \dots, (\widetilde{\boldsymbol{\varepsilon}}, \widetilde{\boldsymbol{\sigma}})_{n_{\mathcal{D}_{\mathrm{loc}}}} \right\} . \tag{1}$$

The set $\mathcal{D}_{\mathrm{loc}}$ can be an arbitrary subset of $\mathcal{D} \subset L^2(\Omega, \mathbb{R}^2 \times \mathbb{R}^2) \times L^2(\Omega, \mathbb{R}^2 \times \mathbb{R}^2)$ and contains a total number of $n_{\mathcal{D}_{\mathrm{loc}}}$ matching pairs of stress states $\widetilde{\boldsymbol{\sigma}}$ and strain states $\widetilde{\boldsymbol{\varepsilon}}$. In this context, "matching" means that these are obtained via experiments or conventional material models. Each pair of stress and strain is called a *material state*. In addition to these material states, the *mechanical states* are defined as

$$\mathcal{E} := \{ (\boldsymbol{\varepsilon}, \boldsymbol{\sigma}) \,|\, -\operatorname{div}(\boldsymbol{\sigma}) = \boldsymbol{f}, \boldsymbol{\varepsilon} = \nabla^{\mathrm{sym}} \boldsymbol{u} \} . \tag{2}$$

More precisely speaking, $\mathcal{E} \subset L^2(\Omega, \mathbb{R}^2 \times \mathbb{R}^2) \times L^2(\Omega, \mathbb{R}^2 \times \mathbb{R}^2)$ reflects all stress states which fulfill equilibrium of forces, and all strain states that are symmetrized gradient fields with respect to the displacement $\boldsymbol{u}$ such that kinematic compatibility is fulfilled. It is important to note that these states of stresses and strains here are not yet connected in any way. The key quantity which links these states of stresses and strains to each other is the *distance function*

$$d^2\left((\boldsymbol{\varepsilon}, \boldsymbol{\sigma}), \mathcal{D}\right) = \inf_{(\widetilde{\boldsymbol{\varepsilon}}, \widetilde{\boldsymbol{\sigma}}) \in \mathcal{D}_{\mathrm{loc}}} \left\{ \int_{\mathcal{B}} W\left(\boldsymbol{\varepsilon} - \widetilde{\boldsymbol{\varepsilon}}\right) \, \mathrm{d}V + \int_{\mathcal{B}} W^*\left(\boldsymbol{\sigma} - \widetilde{\boldsymbol{\sigma}}\right) \, \mathrm{d}V \right\} , \tag{3}$$

with

$$W(\boldsymbol{\varepsilon}) = \frac{1}{2} \, \boldsymbol{\varepsilon} : \mathbf{E} : \boldsymbol{\varepsilon} = \frac{1}{2} \, \underline{\varepsilon} \cdot \underline{\mathsf{E}} \cdot \underline{\varepsilon} \quad , \quad W^*(\boldsymbol{\sigma}) = \frac{1}{2} \, \boldsymbol{\sigma} : \mathbf{C} : \boldsymbol{\sigma} = \frac{1}{2} \, \underline{\sigma} \cdot \underline{\mathsf{C}} \cdot \underline{\sigma} \quad . \tag{4}$$

Obviously, these two quantities W und W^* may be interpreted as energy densities where $\mathbf{E}$ reflects the fourth order elasticity tensor and $\mathbf{C} = \mathbf{E}^{-1}$ the related compliance tensor. Underlined symbols denote the respective Voigt-type matrix representation of tensors. However, it is important to note that W und W^* are quantities which measure the distance between mechanical and material states. Therefore, $\mathbf{E}$ is not necessarily related to the stiffness of a material, but rather contains weighting factors. The quantity $d^2\left((\boldsymbol{\varepsilon}, \boldsymbol{\sigma}), \mathcal{D}\right)$ as defined in (3) is to be interpreted as follows: Provided that the mechanical state $(\boldsymbol{\varepsilon}, \boldsymbol{\sigma})$ is known or fixed for the time being, $d\left((\boldsymbol{\varepsilon}, \boldsymbol{\sigma}), \mathcal{D}\right)$ measures the distance between this mechanical state and the material state, which is closest to it. However, the mechanical states are in general also unknown. They are determined by the assumption of minimizing the distance subject to mechanical equilibrium and kinematic compatibility. This leads to

$$d^2\left((\boldsymbol{\varepsilon}, \boldsymbol{\sigma}), \mathcal{D}\right) = \inf_{(\boldsymbol{\varepsilon}, \boldsymbol{\sigma}) \in \mathcal{E}} \inf_{(\widetilde{\boldsymbol{\varepsilon}}, \widetilde{\boldsymbol{\sigma}}) \in \mathcal{D}_{\mathrm{loc}}} \left\{ \int_{\mathcal{B}} W\left(\boldsymbol{\varepsilon} - \widetilde{\boldsymbol{\varepsilon}}\right) \, \mathrm{d}V + \int_{\mathcal{B}} W^*\left(\boldsymbol{\sigma} - \widetilde{\boldsymbol{\sigma}}\right) \, \mathrm{d}V \right\} . \tag{5}$$

This double minimization problem defines the point of departure for the derivation of the related governing equations and the implementation of the data-based algorithm, both of which will be discussed in the subsequent subsections.

2.2 Governing equations

The basis for the derivation of governing equations and the data-based algorithm is given by (5). These equations, which follow from the constrained minimization with respect to the mechanical states $(\boldsymbol{\varepsilon}, \boldsymbol{\sigma}) \in \mathcal{E}$, shall here be presented in a concise way without consistent derivations (and using a slightly different notation). For further details we refer to, e.g., [1,7]. The derivation of governing equations goes along with the discretization of the underlying physical field variables and the body under consideration. As far as this aspect is concerned, the data-driven approach is identical to the standard Finite Element Method. As primary variable, the array

$$\underline{u} = \begin{bmatrix} u_1^1 & u_2^1 & u_3^1 & u_1^2 & u_2^2 & u_3^2 & \dots & u_1^{n_{\mathrm{np}}} & u_2^{n_{\mathrm{np}}} & u_3^{n_{\mathrm{np}}} \end{bmatrix}^{\mathrm{t}} \tag{6}$$

of node displacements is introduced, where the lower index refers to the spatial coordinates $\boldsymbol{x} = x_i \, \boldsymbol{e}_i$ based on a fixed Cartesian frame, and the upper index refers to the node points of the chosen mesh, the total number of which is n_{np}. For lower-dimensional spatial settings, the coordinates reduce in a straight-forward way considering only two or one displacement coordinates per node. The mechanical state is now parameterized in $\underline{u}$ via

$$\underline{\varepsilon}_q^e = \underline{B}_q^e \, \underline{u} \tag{7}$$

rather than using strains as variables in order to directly fulfill kinematic compatibility. Here, the index e refers to a specific finite element and q to the respective quadrature points. The quantity $\underline{B}_q^e$ denotes matrices which encode the geometry of the

© 2023 The Authors. *Proceedings in Applied Mathematics & Mechanics* published by Wiley-VCH GmbH.

16177061, 2023, 1, Downloaded from https://onlinelibrary.wiley.com/doi/10.1002/pamm.202200206 by Technical University Dortmund, Wiley Online Library on [16/10/2023]. See the Terms and Conditions (https://onlinelibrary.wiley.com/terms-and-conditions) on Wiley Online Library for rules of use; OA articles are governed by the applicable Creative Commons License

structure as well as the connectivity between global nodes and local element nodes. In line with [1], a constrained minimization problem can be derived which yields the stationarity conditions

$$\underline{K}^{NN}\,\underline{u}^{N} + \underline{K}^{ND}\,\underline{u}^{D} = \underline{\mathcal{E}}^{N}\,, \tag{8}$$

$$\underline{\mathsf{C}}\,(\underline{\sigma}_q^e - \widetilde{\underline{\sigma}}_q^{\,e}) - \underline{B}_q^e\,\underline{\eta} = \underline{0}\,, \tag{9}$$

$$\underline{f}_{\mathrm{ext}}^{N} - \underline{f}_{\mathrm{int}}^{N} = \underline{0}\,. \tag{10}$$

The quantities $\underline{K}^{NN}$, $\underline{K}^{ND}$, $\underline{\mathcal{E}}^{N}$ and $\underline{f}_{\mathrm{int}}^{N}$ stem from a conventional redistribution of the global matrices

$$\underline{K} := \sum_{e=1}^{n_{\mathrm{el}}} \sum_{q=1}^{n_{\mathrm{qp}}} w_q^e\,\det(\underline{J}_q^e)\,[\underline{B}_q^e]^{\mathrm{t}}\,\underline{\mathsf{E}}\,\underline{B}_q^e\,, \tag{11}$$

$$\underline{\mathcal{E}} := \sum_{e=1}^{n_{\mathrm{el}}} \sum_{q=1}^{n_{\mathrm{qp}}} w_q^e\,\det(\underline{J}_q^e)\,[\underline{B}_q^e]^{\mathrm{t}}\,\underline{\mathsf{C}}\,\widetilde{\underline{\varepsilon}}_q^{\,e}\,, \tag{12}$$

$$\left[\underline{f}_{\mathrm{int}}\right]^{\mathrm{t}} := \sum_{e=1}^{n_{\mathrm{el}}} \sum_{q=1}^{n_{\mathrm{qp}}} w_e^q\,\det(\underline{J}_q^e)\,\left[\underline{B}_q^e\right]^{\mathrm{t}}\,\underline{\sigma}_q^e\,, \tag{13}$$

by distinguishing entries related to Neumann (N) and Dirichlet (D) boundary conditions. Analogously, $\underline{u}^{N}$ and $\underline{u}^{D}$ are constructed on the basis of the global array introduced in (6). Furthermore, w_q^e denote the coefficients associated to the Gauss quadrature and $\underline{J}_q^e$ is the Jacobian related to the standard coordinate transformation between real physical coordinates and the ones used for the reference element. While $\widetilde{\underline{\varepsilon}}_q^{\,e}$ and $\widetilde{\underline{\sigma}}_q^{\,e}$ are the Voigt representation of stress and strain states picked from the data set in each quadrature point, the (mechanical) stress states $\underline{\sigma}_q^e$ represent additional unknowns. The same applies to the quantity $\underline{\eta}$ which represents Lagrange parameters in order to fulfill equilibrium of forces, cf. (6). The array $\underline{f}_{\mathrm{ext}}$ includes prescribed forces at the nodes. This system of equations can further be reduced by combining (9) and (10) which yields

$$\underline{K}^{NN}\,\underline{u}^{N} + \underline{K}^{ND}\,\underline{u}^{D} = \underline{\mathcal{E}}^{N}\,, \tag{14}$$

$$\underline{K}^{NN}\,\underline{\eta}^{N} = \underline{f}_{\mathrm{ext}}^{N} - \underline{\Sigma}^{N}\,, \tag{15}$$

with $\underline{\Sigma}^{N}$ obtained from

$$\underline{\Sigma} := \sum_{e=1}^{n_{\mathrm{el}}} \sum_{q=1}^{n_{\mathrm{qp}}} w_q^e\,\det(\underline{J}_q^e)\,[\underline{B}_q^e]^{\mathrm{t}}\,\widetilde{\underline{\sigma}}_q^{\,e}\,. \tag{16}$$

Equations (14) and (15) define the final form of the governing equations. However, (9) is still used as an update rule for the local stress states, namely

$$\underline{\sigma}_q^e = \widetilde{\underline{\sigma}}_q^{\,e} + \underline{\mathsf{C}}^{-1}\,\underline{B}_q^e\,\underline{\eta}\,. \tag{17}$$

2.3 Algorithm

As indicated above, the minimization with respect to the mechanical states is performed by assuming the material states fixed. To determine those, a staggered scheme is introduced in [1]. To be more precise, the sequence of steps which defines the algorithm is given by the following scheme:

1. Initialize $(\widetilde{\underline{\varepsilon}}_q^{*e}, \widetilde{\underline{\sigma}}_q^{*e}) \in \mathcal{D}_{\mathrm{loc}}$, e.g. randomly
2. Calculate $\underline{u}^{N}$, $\underline{\eta}^{N}$ via (14) and (15)
3. Calculate mechanical states via (7) and (17)
4. Update material states via (3)
5. If identical values are consecutively chosen for all e and q respectively, goto 6, otherwise goto 2
6. Set mechanical states $(\underline{\varepsilon}_q^e, \underline{\sigma}_q^e)$ as solution

3 Case studies

The following case studies are intended to emphasize specific observations, ideas, and conclusions that emerged during our research activities.

© 2023 The Authors. *Proceedings in Applied Mathematics & Mechanics* published by Wiley-VCH GmbH.

16177061, 2023, 1, Downloaded from https://onlinelibrary.wiley.com/doi/10.1002/pamm.202200206 by Technical University Dortmund, Wiley Online Library on [16/10/2023]. See the Terms and Conditions (https://onlinelibrary.wiley.com/terms-and-conditions) on Wiley Online Library for rules of use; OA articles are governed by the applicable Creative Commons License

3.1 Homogeneous one-dimensional example

First, the general influence of chosen initial values on the calculation of the first mechanical states is discussed in terms of a simple example. Consider a truss member of length l that is subjected to an external load F at one tip. At the other tip, a displacement of zero is prescribed. Two Gauss points shall be used for the calculation and the two tips of the truss member also represent the nodes of the underlying spatial discretization. The elastic constants of the material shall be E in terms of its Young's modulus and, as a consequence, $\mathsf{C} := \mathsf{E}^{-1}$ as compliance. The cross-section area of the truss member is given by A. Now, let $\widetilde{\sigma}_1$, $\widetilde{\sigma}_2$, $\widetilde{\varepsilon}_1$ and $\widetilde{\varepsilon}_2$ be the initially and randomly chosen material states in the two Gauss points. Then, the solution of (14) and (15) results in

$$u^2 = \frac{\widetilde{\varepsilon}_1 + \widetilde{\varepsilon}_2}{2}\, l \quad , \quad \eta^2 = \frac{1}{\mathsf{C}} \left[\frac{F\, l}{A} - \frac{\widetilde{\sigma}_1 + \widetilde{\sigma}_2}{2}\, l \right] \tag{18}$$

for node number 2, where the prescribed force F is applied. The mechanical states are then given by

$$\varepsilon_1 = \varepsilon_2 = \frac{\widetilde{\varepsilon}_1 + \widetilde{\varepsilon}_2}{2} \quad , \quad \sigma_1 = \frac{F}{A} + \frac{\widetilde{\sigma}_1 - \widetilde{\sigma}_2}{2} \quad , \quad \sigma_2 = \frac{F}{A} + \frac{\widetilde{\sigma}_2 - \widetilde{\sigma}_1}{2} \, . \tag{19}$$

The aim of this example is to explicitly show the influence of the initially chosen material states at least on the mechanical states calculated first. There are also two main takeaways: (i) The influence on the stress states would vanish here if identical initial stress values are chosen from $\mathcal{D}_{\mathrm{loc}}$ and the exact solution is obtained, (ii) the average of the two local stress states yield the exact solution independent of the material states. These aspects are revisited and discussed in the following sections.

3.2 Homogeneous two-dimensional example

Prior to the application of the data-driven scheme to complex spatially two-dimensional problems the basic performance in terms of a patch test shall be considered.

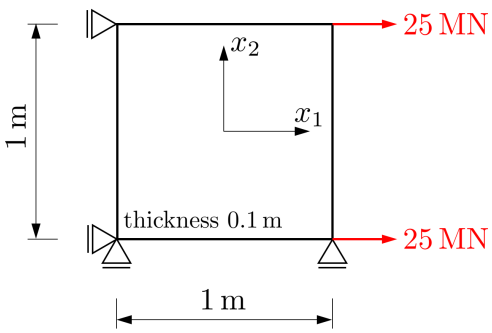

Fig. 1: Patch test using one element.

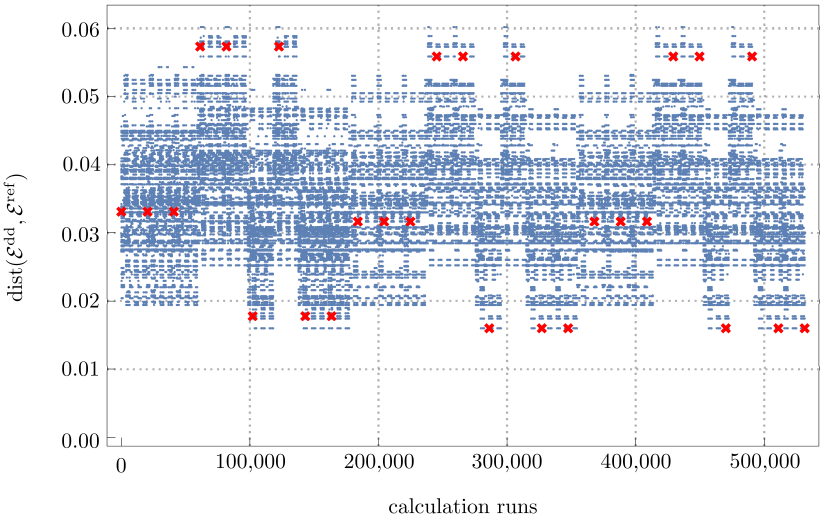

Fig. 2: Accuracy of the results obtained for all 531,441 runs of the patch test.

As shown in Figure 1, a single spatially two-dimensional finite element with four integration points is subjected to singular forces. The boundary values should result in a homogeneous deformation of the square body and homogeneously distributed strains of $[\varepsilon_{11}, \varepsilon_{22}, 2\,\varepsilon_{12}] = [0.002, -0.0009, 0.]$ as well as stresses of $[\sigma_{11}, \sigma_{22}, \sigma_{12}] = [500., 0., 0.]$ MPa. In this example, all possible combinations of initial material states in the four integration points shall be used. Therefore, the data set needs to be rather small. More precisely, a grid which stems from the prescribed values of $\widetilde{\varepsilon}_{11} = [-0.0025, 0., 0.0025]$, $\widetilde{\varepsilon}_{22} = [-0.0025, 0., 0.0025]$ and $2\,\widetilde{\varepsilon}_{12} = [-0.00125, 0., 0.00125]$ is used, resulting in $3^3 = 27$ data set entries and a total of 531,441 possible combinations and thus calculations. The associated stress values are determined by using a standard isotropic elasticity model with 210 GPa as Young's modulus and 0.3 as Poisson's ratio.

Figure 2 shows the accuracy of the results obtained by all 531,441 runs of the patch test. We used the distance $\mathrm{dist}(\mathcal{E}^{\mathrm{dd}}, \mathcal{E}^{\mathrm{ref}})$ according to (3) as measure for the accuracy, where $\mathcal{E}^{\mathrm{dd}}$ refers to the mechanical states obtained by the data-driven approach and $\mathcal{E}^{\mathrm{ref}}$ refers to the reference solution obtained by a conventional FEM calculation. It becomes apparent, that several different results are obtained by the data-driven scheme for different combinations of initial material states. These results differ from each other in terms of local solutions obtained in the integration points (not observable from Fig. 2) and also in terms of accuracy. Furthermore, the discrepancy of obtained accuracy is significant due to the fact that the least accurate solutions

© 2023 The Authors. *Proceedings in Applied Mathematics & Mechanics* published by Wiley-VCH GmbH.

16177061, 2023, 1, Downloaded from https://onlinelibrary.wiley.com/doi/10.1002/pamm.202200206 by Technical University Dortmund, Wiley Online Library on [16/10/2023]. See the Terms and Conditions (https://onlinelibrary.wiley.com/terms-and-conditions) on Wiley Online Library for rules of use; OA articles are governed by the applicable Creative Commons License

correspond to a distance of ≈ 0.060182. This is about 3.75 times larger than the accuracy of the best obtained solutions with a distance of ≈ 0.015992, which is obtained in 1,675 of the 531,441 cases. The conclusion to be drawn from the previous analyses that the choice of identical initial material states should generally lead to more accurate results cannot be sustained. The red colored crosses in Fig. 2 indicate the solutions which were calculated with identically chosen initial material states. Accordingly, the most accurate as well as considerably less accurate results can be obtained. Therefore, a general recommendation cannot be derived from this. It is however important to note, that the average of local mechanical states obtained by the data-driven approach always perfectly coincides with the reference solution. This leads to the conclusion, that one always obtained the optimal solution in an averaged sense, however, the local deviations from this can be rather large.

For comparison, the same problem was solved by using Mixed-Integer Quadratic Program (MIQP) according to [19] and, to be more specific, the IBM ILOG CPLEX Optimization Studio Version 12.10.0 (https://www.ibm.com/de-de/products/ilog-cplex-optimization-studio). With this method, the most accurate results with $\mathrm{dist}(\mathcal{E}^{\mathrm{MIQP}}, \mathcal{E}^{\mathrm{ref}}) \approx 0.015992$ is obtained. Due to the fact that the used routine does not require any initial values, a corresponding analysis of their influence on accuracy is pointless here. This result also shows that the staggered scheme is capable of finding the best possible solution, however only in $\approx 0.32\%$ of the calculations.

3.3 Inhomogeneous two-dimensional example

As a conclusion of the case studies discussed in the previous section, MIQP seems to provide a sophisticated method in conjunction with the data-driven scheme. Therefore, the capabilities of MIQP shall further be analyzed in terms of the simulation of the behavior of a notched plate subjected to a distributed load, cf. Fig. 3. Shown here is the distribution of the discrepancy between the mechanical states obtained by MIQP and the reference solution obtained by a standard FE approach in terms of

$$\sigma_{\mathrm{local}}^{\mathrm{RMS}} = \left[\frac{W^*(\boldsymbol{\sigma}_q^{e,\mathrm{MIQP}} - \boldsymbol{\sigma}_q^{e,\mathrm{ref}})}{W^*(\boldsymbol{\sigma}_q^{e,\mathrm{ref}})} \right]^{\frac{1}{2}} . \tag{20}$$

In this example, the data set is again generated by using a standard linear elastic material model with the parameters indicated above and the same coarse data set is used except that the prescribed shear strains are chosen within the range $2\widetilde{\varepsilon}_{12} = [-0.0025, 0., 0.0025]$. The spatial discretization includes nine elements which is obviously rather coarse. The reason for choosing the very coarse data set and discretization is that the solution of the problem at hand already takes about 13.5 hours. While MIQP with an objective value of ≈ 0.004 delivers substantially more accurate results (in average) in comparison to the conventional staggered algorithm with ≈ 0.027 as objective value (corresponds to $\approx 675\,\%$ less accuracy), the latter with approx. 6 seconds is $\approx 809,900\,\%$ faster than MIQP.

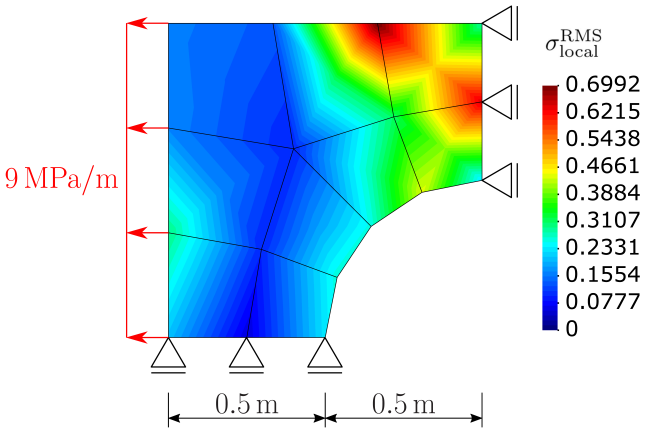

Fig. 3: Distribution of local error obtained by MIQP, cf. (20).

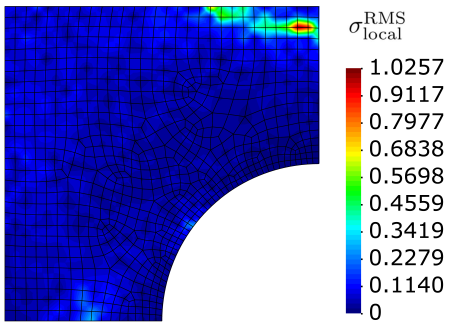

Fig. 4: Local errors obtained by the staggered scheme, cf. (20).

This enables the conventional method to be applied to much more complex problems in terms of finer discretizations and higher data set densities. Fig. 4 shows the results of the conventional algorithm to the identical problem as before, however using 836 elements and $75^3 = 421,875$ data set entries which cover the same ranges of prescribed strain values as before, however divided into 75 equidistant increments. With the significantly finer spatial discretization and the significantly denser data set at hand, the staggered scheme yields more accurate results than MIQP in the previous example in an averaged sense. While the averaged error based on (20) is ≈ 0.449 in the MIQP example, it is ≈ 0.073 here which corresponds to $\approx 16.3\,\%$. However, the local variations can be rather large as they exceed $100\,\%$ in specific regions of the structure.

© 2023 The Authors. *Proceedings in Applied Mathematics & Mechanics* published by Wiley-VCH GmbH.

16177061, 2023, 1, Downloaded from https://onlinelibrary.wiley.com/doi/10.1002/pamm.202200206 by Technical University Dortmund, Wiley Online Library on [16/10/2023]. See the Terms and Conditions (https://onlinelibrary.wiley.com/terms-and-conditions) on Wiley Online Library for rules of use; OA articles are governed by the applicable Creative Commons License

4 Summary

Although data-driven mechanics exhibits great potential for future wide-ranging applications, significant problems are inherent in this new method. The influence of the choice of initial material states on the accuracy of the results obtained with the original data-driven algorithm is generally very significant. An explicit representation of this influence can be obtained for simple examples such as a truss member with two integration points, at least with respect to the calculation of the first mechanical state. Possible conclusions drawn from this basic examples are to use identical initial values for the material states in each integration point. However, this conclusion could not be maintained after analyzing the patch test results. In this example, no obvious relation could be found between the chosen initial values and the accuracy of the final results. It was found that the original algorithm obviously tends to have solutions dwell in local minima of the distance function. These numerous local states can differ significantly from each other in terms of stress and strain states as well as accuracy. The volume averages of related physical fields with respect to single finite elements always yield much more accurate results or even exact solutions where applicable. Nevertheless, this cannot be regarded as an appropriate workaround since the prediction of load-bearing capacities relies on minimal/maximal local stress states and not average values. It can be stated — without providing a rigorous mathematical proof here — that these drawbacks are caused by the staggered implementation of the double and nested minimization problem at hand. The treatment of the underlying problem via MIQP yields very promising results. However, this method seems only applicable to problems with very few degrees of freedom referring both to the spatial discretization as well as data set density. This makes MIQP rather inapplicable for data-driven schemes in solid mechanics. The conventional staggered minimization scheme is significantly faster which allows to treat problems with a reasonable number of degrees of freedoms. However as discussed above, the local variation in accuracy appears to be difficult to control and influence with the conventional method.

Based on the results and analysis presented here, it is concluded that the conventional method should be extended in the sense of avoiding so many local minima of the distance function. MIQP represents a theoretically optimal implementation, but due to its inefficiency, it is not applicable to perform representative simulations. Therefore, the next goal is to develop suitable enhancements to the distance function and/or the minimization algorithm accordingly.

Acknowledgements The financial support by the German Research Foundation (DFG) through the Priority Programme 2256: "Variational Methods for Predicting Complex Phenomena in Engineering Structures and Materials", project 3 (project number 440942664), is gratefully acknowledged. Open access funding enabled and organized by Projekt DEAL.

References

[1] T. Kirchdoerfer and M. Ortiz, Computer Methods in Applied Mechanics and Engineering **304**, 81–101 (2016).
[2] R. Ibanez, E. Abisset-Chavanne, J. V. Aguado, D. Gonzalez, E. Cueto, and F. Chinesta, Archives of Computational Methods in Engineering **25**(1), 47–57 (2018).
[3] T. Kirchdoerfer and M. Ortiz, Computer Methods in Applied Mechanics and Engineering **326**, 622–641 (2017).
[4] T. Kirchdoerfer and M. Ortiz, International Journal for Numerical Methods in Engineering **113**(11), 1697–1710 (2018).
[5] L. Stainier, A. Leygue, and M. Ortiz, Computational Mechanics **64**(2), 381–393 (2019).
[6] M. Bessa, R. Bostanabad, Z. Liu, A. Hu, D. W. Apley, C. Brinson, W. Chen, and W. K. Liu, Computer Methods in Applied Mechanics and Engineering **320**, 633–667 (2017).
[7] L. T. K. Nguyen and M. A. Keip, Computers & Structures **194**, 97–115 (2018).
[8] S. Conti, S. Müller, and M. Ortiz, Archive for Rational Mechanics and Analysis **229**(1), 79–123 (2018).
[9] S. Conti, S. Müller, and M. Ortiz, Archive for Rational Mechanics and Analysis **237**, 1–33 (2020).
[10] Q. He and J. S. Chen, Computer Methods in Applied Mechanics and Engineering **363**, 112791 (2020).
[11] R. Xu, J. Yang, W. Yan, Q. Huang, G. Giunta, S. Belouettar, H. Zahrouni, T. B. Zineb, and H. Hu, Computer Methods in Applied Mechanics and Engineering **363**, 112893 (2020).
[12] K. Karapiperis, L. Stainier, M. Ortiz, and J. Andrade, Journal of the Mechanics and Physics of Solids **147**, 104239 (2021).
[13] F. Feyel and J. L. Chaboche, Computer Methods in Applied Mechanics and Engineering **183**(3-4), 309–330 (2000).
[14] R. Eggersmann, T. Kirchdoerfer, S. Reese, L. Stainier, and M. Ortiz, Computer Methods in Applied Mechanics and Engineering **350**, 81–99 (2019).
[15] K. Ciftci and K. Hackl, Computational Mechanics **70**, 425–435 (2022).
[16] K. Poelstra, T. Bartel, and B. Schweizer, A data driven framework for evolutionary problems in solid mechanics, preprint available at http://www.mathematik.tu-dortmund.de/lsi/schweizer/Preprints/Data-driven-plasticity-preprint-2021.pdf, November 2021.
[17] L. T. K. Nguyen, M. Rambausek, and M. A. Keip, Computer Methods in Applied Mechanics and Engineering **365**, 112898 (2020).
[18] R. Eggersmann, L. Stainier, M. Ortiz, and S. Reese, Computer Methods in Applied Mechanics and Engineering **373**, 113499 (2021).
[19] Y. Kanno, Optimization Letters **13**(7), 1505–1514 (2019).

© 2023 The Authors. *Proceedings in Applied Mathematics & Mechanics* published by Wiley-VCH GmbH.

16177061, 2023, 1, Downloaded from https://onlinelibrary.wiley.com/doi/10.1002/pamm.202200206 by Technical University Dortmund, Wiley Online Library on [16/10/2023]. See the Terms and Conditions (https://onlinelibrary.wiley.com/terms-and-conditions) on Wiley Online Library for rules of use; OA articles are governed by the applicable Creative Commons License